Effect of molybdenum on continuous cooling transformations in two medium carbon forging steels

C. GARCÍA DE ANDRÉS
Department of Physical Metallurgy, Centro Nacional de Investigaciones Metalúrgicas (CENIM), Consejo Superior de Investigaciones Científicas (CSIC), Avda. Gregorio del Amo, 8. 28040 Madrid, Spain
E-mail: cgda@cenim.csic.es

C. CAPDEVILA, F. G. CABALLERO
Department of Physical Metallurgy, Centro Nacional de Investigaciones Metalúrgicas (CENIM), Consejo Superior de Investigaciones Científicas (CSIC), Avda. Gregorio del Amo, 8. 28040 Madrid, Spain; Phase Transformations & Complex Properties Research Group, Department of Materials Science and Metallurgy, University of Cambridge, Pembroke Street, Cambridge CB2 3QZ, UK

D. SAN MARTÍN
Department of Physical Metallurgy, Centro Nacional de Investigaciones Metalúrgicas (CENIM), Consejo Superior de Investigaciones Científicas (CSIC), Avda. Gregorio del Amo, 8. 28040 Madrid, Spain

Continuous cooling transformations in two medium carbon microalloyed forging steels have been studied. The influence of austenite grain size and molybdenum content on diffusion-controlled transformations and displacive transformations has been thoroughly analyzed. Moreover, a study of the austenite grain structure previous to the transformation has been carried out. In this sense, the evolution of austenite grain size with austenitization temperature has been experimentally analyzed. That allowed to detect the temperature at which an undesirable microstructure with a duplex grain morphology starts to form. Finally, continuous cooling conditions to reach a final microstructure formed mainly of acicular ferrite in industrial forging processes has been determined.
© *2001 Kluwer Academic Publishers*

1. Introduction
Significant efforts have been recently devoted to investigate medium carbon microalloyed forging steels with cooper and manganese sulfides in order to induce the formation of acicular ferrite for toughness improvement [1–6]. These efforts are driven by the need to develop alloys for the automotive industries and offshore oil and gas industries; some of them are required for service in hostile environments. However, a better understanding of the role of alloying elements and parameters, such as austenite grain size, should be achieve to produce this kind of steels [2, 6–10].

Ito *et al.* [9] argued that acicular ferrite is intragranularly nucleated bainite. The morphologies of acicular ferrite and conventional bainite differ in that the former nucleates intragranularly at inclusions inside large austenite grains, whereas in steels relatively free of non-metallic inclusions, bainite nucleates initially in austenite/austenite grain surfaces and grows by repeated formation of sub-units to generate the classical sheaf morphology. Experimental data reported by Harrison and Farrar [11] show that conventional bainite or acicular ferrite can be obtained under identical isothermal transformation conditions in the same steel. Nevertheless, a small austenite grain size enhances bainite formation since the majority of nucleation events occur at the austenite grain surfaces. Subsequent growth then swamps the interiors of the austenite grains, preventing the formation of acicular ferrite. Whereas, in the case of large austenite grains, the number density of intragranular nucleation sites (inclusions) is significant enough to form acicular ferrite in preference to bainite. By contrast, some studies have demonstrated that in steels containing appropriate inclusions, the acicular ferrite can be obtained during the isothermal decomposition of austenite irrespective of prior austenite grain size (PAGS) [6].

It has been recently demonstrated that medium carbon microalloyed forging steels with acicular ferrite microstructure can be reliably manufactured under continuous cooling in large quantities with obvious interest for the good combination of mechanical

properties [5]. The purpose of the present work is to study the continuous cooling transformations of two medium carbon microalloyed forging steels with different molybdenum content and two very different PAGSs. Moreover, an attempt has been made to reach a final microstructure formed mainly of acicular ferrite by industrial continuous cooling.

2. Experimental procedure

Two medium carbon microalloyed forging steels with different molybdenum content have been studied. Their actual chemical composition is listed in Table I. Alloys were prepared as a 2500 kg vacuum induction melt from high purity base material. After casting and cropping, ingots were hot rolled down to a 50 mm square bar.

Cylindrical dilatometric samples of 2 mm in diameter and 12 mm in length were machined longitudinally to rolling direction. An Adamel Lhomargy DT1000 high-resolution dilatometer has been used to analyze non-isothermal transformations and to determine the continuous cooling transformation diagrams (CCT) of these steels. The dilatometer is equipped with a radiation furnace for heating. The heat radiated by two tungsten filament lamps is focussed on the specimen by means of a bi-elliptical reflector. The temperature is measured with a 0.1 mm diameter type-K Chromel-Alumel thermocouple spot welded to the specimen. Cooling is performed by helium flow directly blow onto the sample surface. The helium flow-rate during cooling is controlled by a proportional servo-valve. The excellent efficiency of heat transmission and the very low thermal inertia of the system ensure that the heating and cooling rates ranging from 0.003 °C/s to 200 °C/s remain constant. The dimensional variations of the specimen are transmitted via an amorphous silica push-rod. These variations are measured by a linear variable differential transformer (LVDT) sensor in a gas-tight enclosure enabling testing under vacuum or in an inert atmosphere. The dilatometric curve is monitored along the thermal cycle with the help of a computer assisted electronic device.

The heating and cooling devices of this dilatometer have been also used to determine the evolution of PAGS with austenitization temperature. Dilatometric specimens were austenitized at a constant heating rate of 5 °C/s at temperatures ranging from 950 to 1250 °C. Finally, specimens were gas quenched to room temperature.

Specimens were ground and polished by standardized techniques, and subsequently etched with picric reagent (2 g picric acid + 50 ml of Teepol + a few drops of hydrochloric acid). Mean prior austenite grain diameter (PAGD) was measured using a linear intercept method [12]. The distribution of PAGD at different austenitization temperatures for the studied steels was obtained using a Kontron IBAS 2 automatic image analyzer [13].

All specimens tested to determine CCT diagrams were etched with 2% Nital solution for optical microstructural characterization. Volume fraction of the different phases present in the microstructure was estimated by an unbiased systematic manual point counting procedure based upon stereological principles [14].

3. Results and discussion

In order to fix the austenitization conditions for the determination of CCT diagrams at two extreme mean PAGD, the variation of this parameter with the austenitization temperature has been studied. Table II shows experimental results of mean PAGD of the two studied steels.

3.1. Distribution of prior austenite grain size

In a normal austenite grain growth, the distribution of grain sizes should be roughly uniform. However, in some cases, certain grains might grow excessively leading to a duplex austenite grain microstructure. Several authors reported that the non-homogeneous dissolution and coarsening of second phase particles could enhance a duplex grain growth during austenitization [15–18].

It should be noticed that duplex grain microstructure would not be recognized if only mean grain size results (Table II) were given. For this reason, a more careful determination of the PAGD has been carried out by means of image analysis. Fig. 1 shows the distribution of PAGD in steels A and B at different austenitization temperatures.

TABLE I Actual chemical composition (wt %) of studied steels

Steel	C	Mn	Si	P	S	Cr	Mo	V	Cu	Al	Ti	N
A	0.37	1.45	0.56	0.010	0.043	0.04	0.025	0.11	0.14	0.024	0.015	0.0162
B	0.38	1.44	0.62	0.010	0.041	0.07	0.16	0.10	0.07	0.026	0.016	0.0122

TABLE II Mean PAGD

Steel A							
Temperature, °C	950	1000	1050	1100	1150	1200	1250
PAGD, μm	8 ± 1	11 ± 1	27 ± 3	33 ± 5	53 ± 2	66 ± 9	72 ± 7

Steel B								
Temperature, °C	950	975	1000	1075	1100	1125	1150	1200
PAGD, μm	12 ± 1	13 ± 2	14 ± 1	45 ± 9	52 ± 8	68 ± 16	102 ± 23	132 ± 38

Figure 2 Duplex austenite microstructure at (a) 1250°C in steel A and (b) 1150°C in steel B.
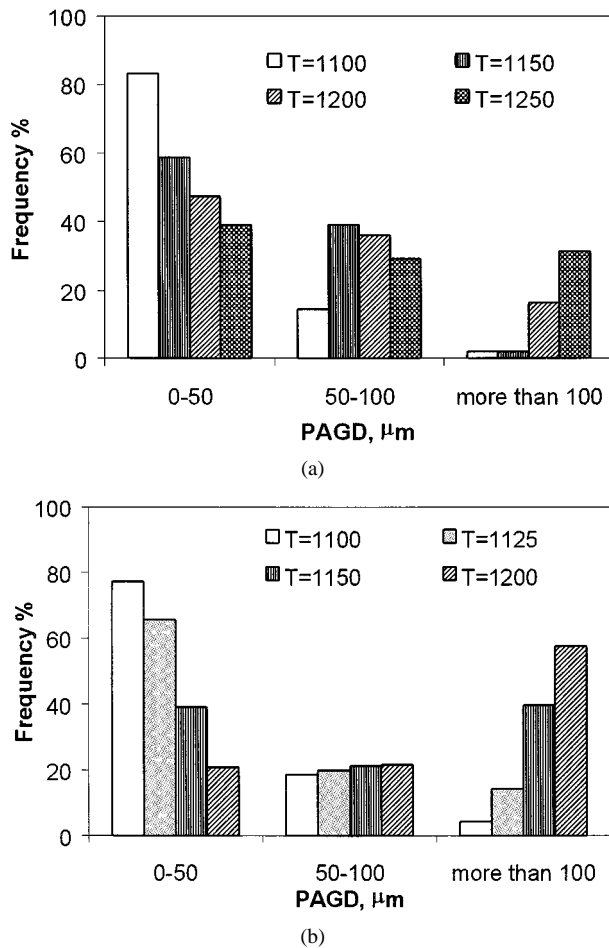
Figure 1 Distribution of austenite grain diameters at different austenitization temperatures for (a) steel A and (b) steel B.

A duplex austenite grain microstructure usually exhibits a bimodal frequency distribution of grain diameters. In this work, it is considered that a duplex microstructure is formed when the frequency of small grains (PAGD smaller than 50 μm) and large grains (PAGD higher than 100 μm) is simultaneously more than 10%. In this sense, Fig. 1 suggests that a duplex grain microstructure is formed at temperatures higher than 1200 °C in steel A and higher than 1125 °C in steel B.

Fig. 2 shows microstructures with a duplex grain morphology for both steels. These micrographs correspond to the most extreme cases of duplex microstructure found in this work.

3.2. Continuous cooling transformation (CCT) diagrams

Continuous cooling transformation diagrams have served an incredibly useful purpose in representing the transformation characteristics of steels not isothermally heat treated, and in revealing the role of alloying elements in influencing the microstructures of the steels. With regards to the decomposition of austenite, these diagrams can be divided, at least, into two separate C-curves, one of which represents reconstructive transformations (polygonal ferrite, i.e. allotriomorphic and/or idiomorphic ferrite, and pearlite) and the other, displacive reactions (bainite and/or acicular ferrite) [19].

With the aim of studying the influence of prior austenite grain size on non-isothermal transformations of these steels, CCT diagrams have been obtained for a fine and coarse PAGS. As a fine grain, a PAGD of 11 μm approximately has been selected. Since a duplex austenite microstructure could make more difficult the analysis of non-isothermal transformations in these steels, the coarse grain should be carefully chosen. According to Fig. 1, and Table II, it is selected a PAGD of 67 μm approximately that corresponds to the temperatures at which the duplex morphology starts to be formed. Table III lists the austenitization temperatures required to reach both PAGD in those steels.

Figs 3 and 4 show the CCT diagrams of steels A and B with a mean PAGD of approximately 11 and 67 μm, respectively. In these diagrams PF is polygonal ferrite, P is pearlite, AF is acicular ferrite and/or bainite and M is martensite. In these figures it is evident that the ferrite and pearlite formation areas shift to higher times since a reduction in austenite grain boundary area occurs as austenite grain size increases.

In relation to the reconstructive transformation, these figures also suggest that PF is obtained after decomposition of austenite with a PAGD of 11 μm by continuous cooling at every tested cooling rate for both steels,

TABLE III Austenitization temperatures for CCT diagrams

Steel	Austenitization Temperatures, °C	PAGD, μm
A	1000	11 ± 1
	1200	66 ± 9
B	950	12 ± 1
	1125	68 ± 16

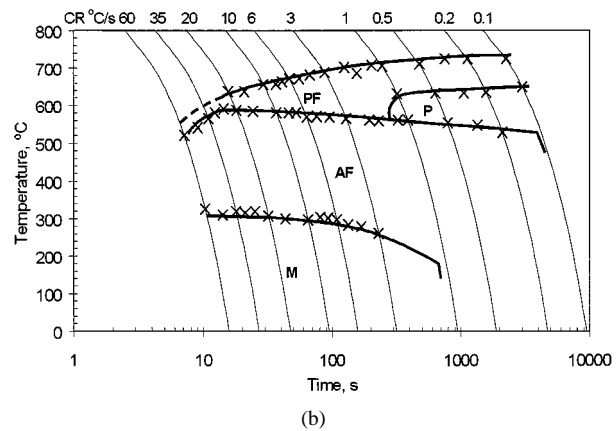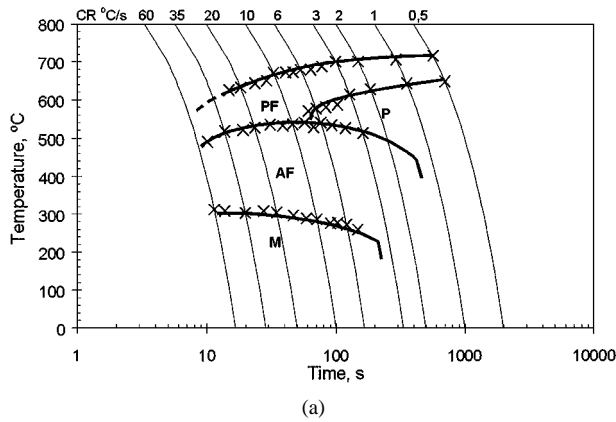*Figure 3* CCT diagrams of (a) steel A (PAGD = 11 μm) and (b) steel B (PAGD = 12 μm).

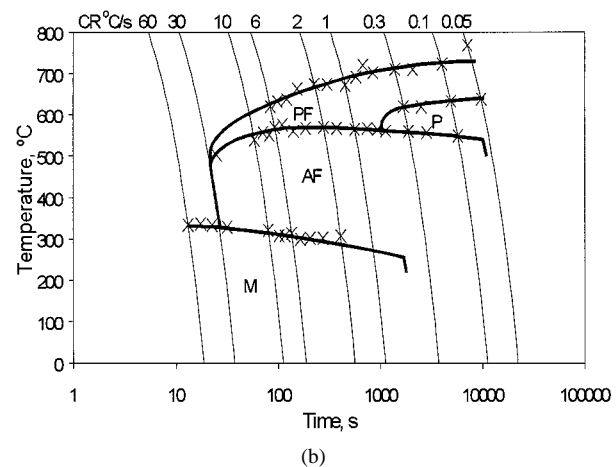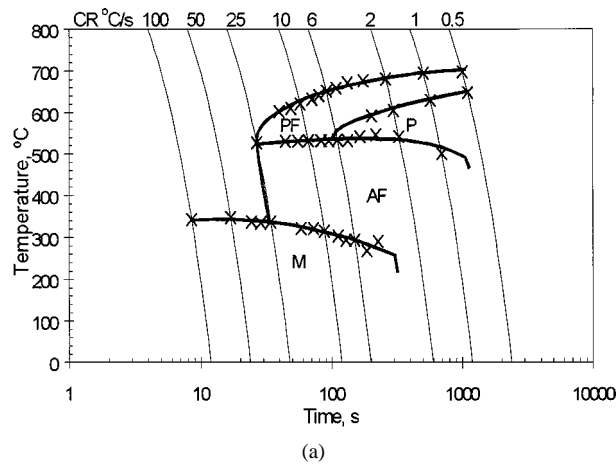*Figure 4* CCT diagrams of (a) steel A (PAGD = 66 μm) and (b) steel B (PAGD = 68 μm).

whereas for a PAGD of 67 μm PF is only formed at cooling rates lower than 25 °C/s in steel A and lower than 30 °C/s in steel B. Moreover, P appears for a PAGD of 11 μm at cooling rates lower than 7.5 °C/s in steel A, and lower than 1.5 °C/s in steel B. However for a PAGD of 67 μm, P is obtained cooling down at rates lower than 6.5 °C/s in steel A and lower than 0.6 °C/s in steel B. The presence of both PF and P in the microstructure are always detrimental for mechanical properties.

Figs 5 and 6 show the variation of start temperatures of austenite-to-ferrite (Ar$_3$) and austenite-to-pearlite (P$_s$) transformations as a function of cooling rates between 800 and 500 °C (CR$_{8/5}$), respectively, of the two steels at both 11 and 67 μm of PAGD. According to these figures, the addition of molybdenum significantly shifts the P$_s$ temperature to lower cooling rates at both PAGDs, but it only slightly affects the Ar$_3$ temperature. This result is consistent with the fact that molybdenum addition delays the beginning of the pearlitic transformation [20].

On the other hand, the anisothermal austenite-to-acicular ferrite transformation for a PAGD of 11 μm occurs at cooling rates higher than 1.5 °C/s in steel A and 0.12 °C/s in steel B. For a PAGD of 67 μm, this transformation takes place at cooling rates ranging from 25 to 0.7 °C/s in steel A and at cooling rates between 30 and 0.07 °C/s in steel B. Therefore, acicular ferrite formation area is reduced and shifted to lower cooling rates as PAGD increases. However, molybdenum content widens the range of cooling rates in which acicular ferrite is formed.
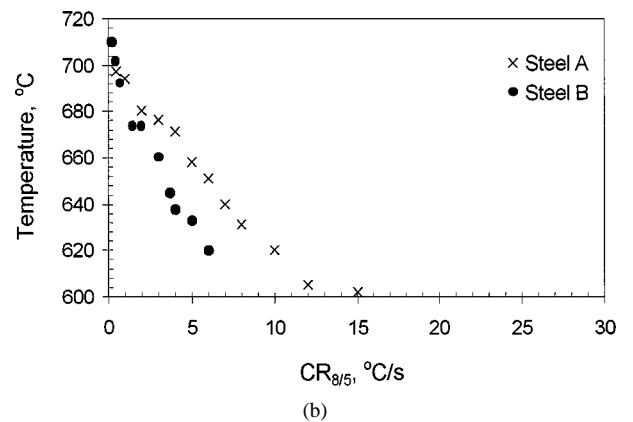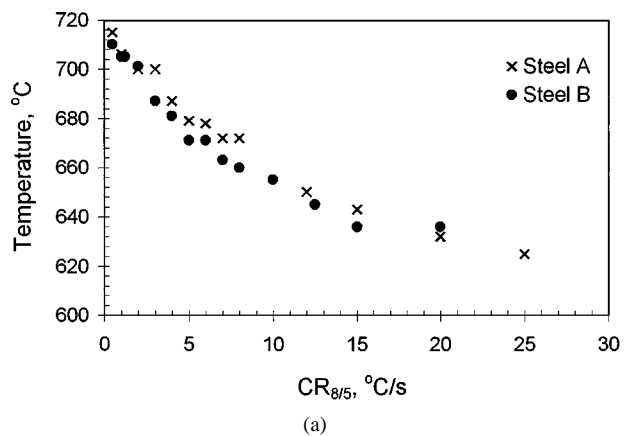

Figure 5 Austenite-to-ferrite start transformation temperatures (Ar$_3$) for a PAGD of (a) 11 μm and a PAGD of (b) 67 μm approximately.
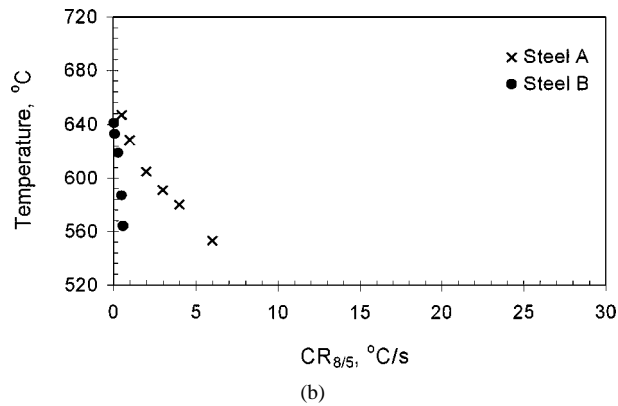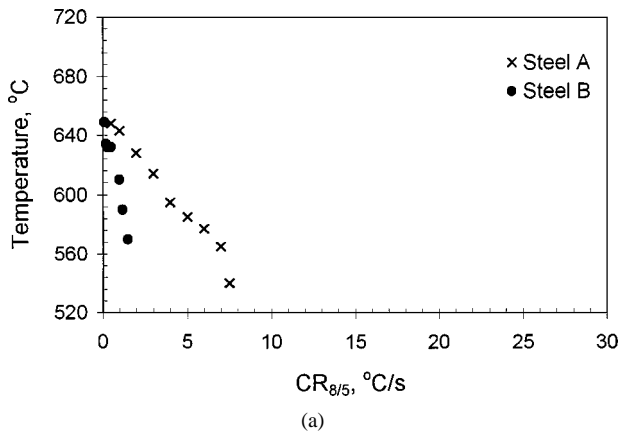
Figure 6 Austenite-to-pearlite start transformation temperatures (P$_s$) for a PAGD of (a) 11 μm and a PAGD of (b) 67 μm approximately.

Cooling rates between 6 and 2 °C/s are possible to be reached at an industrial scale. In this sense, Figs 7 and 8 show microstructures obtained by continuous cooling at rates of 6 and 2 °C/s for both PAGDs in steel A and B, respectively. A reduction of the amount of PF and P is observed in these figures as PAGD and cooling rate increase. Likewise, larger PAGD enhances the transformation austenite-to-acicular ferrite in detriment to reconstructive and bainite transformations [5, 21, 22].

With the aim of obtaining a final microstructure formed mainly of acicular ferrite, a PAGD of 67 μm is the most suitable austenitization condition for these steels. An air cooling in industrial forging processes takes place at a cooling rate of 3 °C/s approximately. That cooling rate is widely used in controlled cooling tunnels of these processes. Fig. 9 shows the microstructures obtained at a cooling rate of 3 °C/s for both steels with a PAGD of 67 μm. In steel A (Fig. 9a), allotriomorphic ferrite decorates the austenite grain boundary and pearlite starts to form around several ferrite grains and residual austenite becomes to transform to AF. The final amount of AF present in the microstructure is 83%. In the molybdenum containing steel (steel B), as it is clearly shown in Fig. 9b, allotriomorphic ferrite is hardly present, pearlite is totally suppressed and AF becomes the main austenite transformation product during cooling at 3 °C/s. The volume fraction of AF in the microstructure is 85% in steel B. By contrast to steel A, martensite is the other phase present in the final
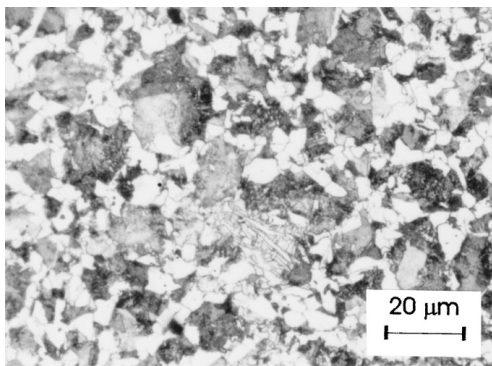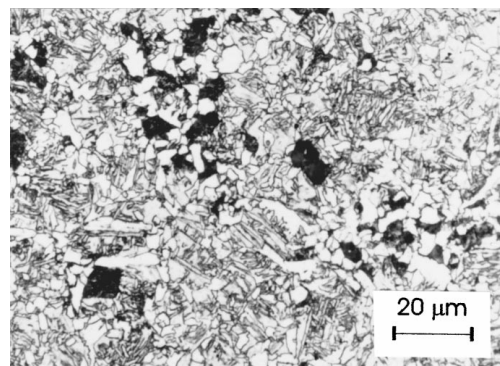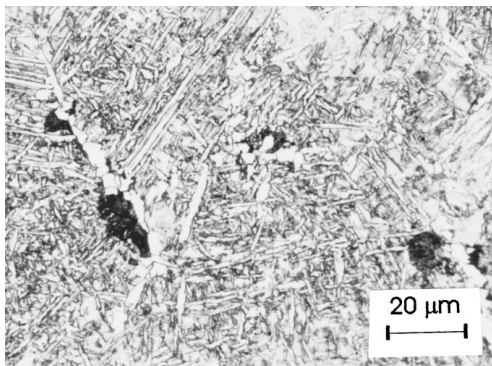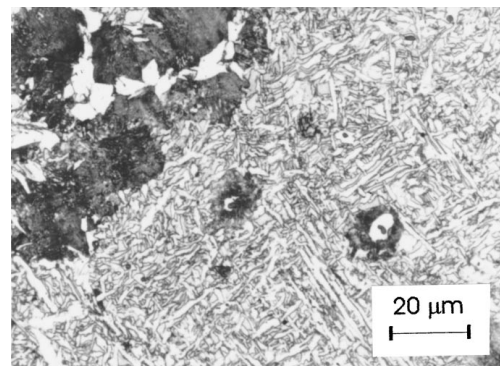

Figure 7 Optical micrographs of microstructures obtained after cooling at 6 and 2°C/s for a PAGD of 11 μm and 67 μm in steel A (a) 6°C/s–11 μm, (b) 2°C/s–11 μm, (c) 6°C/s–67 μm and (d) 2°C/s–67 μm.
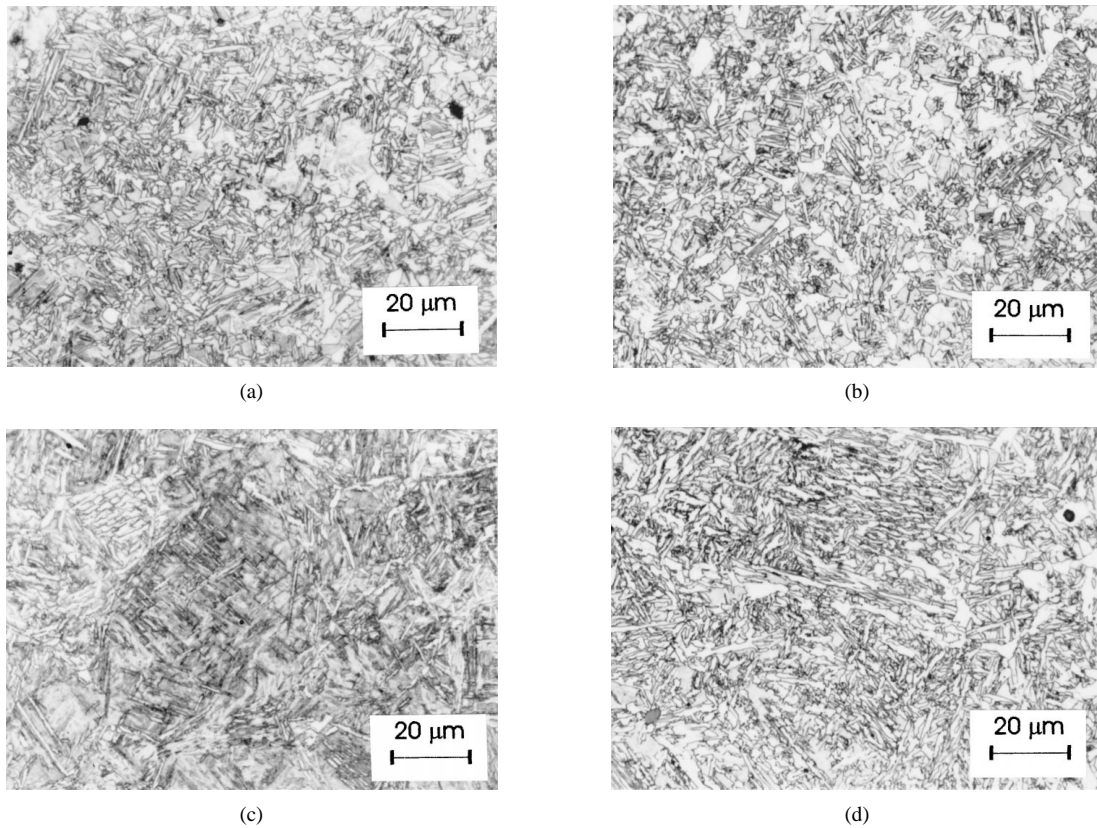
Figure 8 Optical micrographs of microstructures obtained after cooling at 6 and 2°C/s for a PAGD of 11 μm and 67 μm in steel B (a) 6°C/s–11 μm, (b) 2°C/s–11 μm, (c) 6°C/s–67 μm and (d) 2°C/s–67 μm.

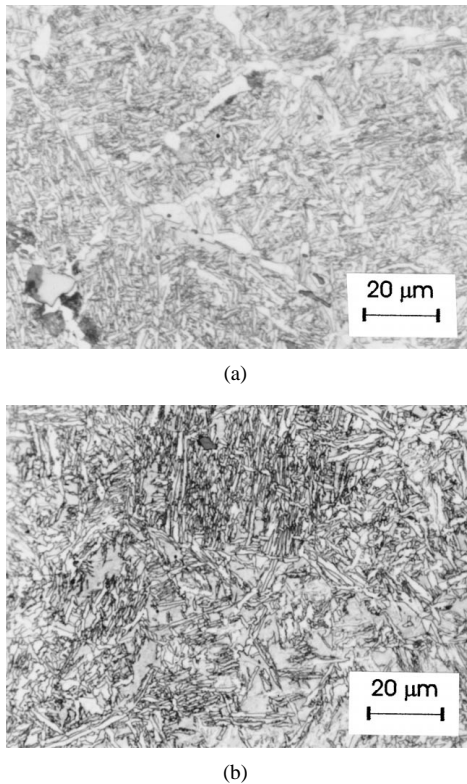*Figure 9* Optical micrographs of microstructures obtained after cooling at 3°C/s in (a) steel A and (b) steel B for a PAGD of 67 μm.

microstructure of the molybdenum containing steel. It would be expected that the microstructure obtained by air cooling in steel B could have a better combination of mechanical properties than that obtained in steel A.

4. Conclusions

1. The distribution of PAGS at different temperatures has been obtained in two medium carbon forging steels with different molybdenum content. An austenite grain microstructure with a duplex morphology has been detected at temperatures higher than 1200 °C in steel A and higher than 1125 °C in steel B.

2. Continuous cooling transformation diagrams for two very different PAGS have been performed for these steels. It has been found that the polygonal ferrite and pearlite formation areas in CCT diagrams shift to longer times as austenite grain size increases. An increase in molybdenum content significantly shifts the start temperature of pearlite transformation to lower cooling rates.

3. A PAGD of approximately 67 μm is advised to obtain a microstructure mainly formed by acicular ferrite in these steels. At a cooling rate of 3 °C/s, easily reproduced in industrial forging processes (air-cooling), a mainly acicular ferrite microstructure is formed in both steels with a PAGD of 67 μm. Allotriomorphic ferrite and pearlite also appear in that microstructure of steel A whereas martensite is present in the microstructure of steel B.

References

1. I. MADARIAGA, J. L. ROMERO and I. GUTIÉRREZ, *Metall. Trans. A* **29A** (1998) 1003.
2. C. GARCÍA DE ANDRÉS, C. CAPDEVILA and F. G. CABALLERO, in Proceedings of the Congreso Nacional de Tratamientos Térmicos y de Superficie TRATERMAT 98, Madrid, May 1998, edited by M. Carsi, F. Peñalba, O. A. Ruano and B. Fernandez (CENIM (CSIC), Madrid, 1998) p. 135.
3. I. MADARIAGA and I. GUTIÉRREZ, *Acta Mater.* **47**(3) (1999) 951.
4. C. GARCÍA DE ANDRÉS, C. CAPDEVILA and F. G. CABALLERO, in Proceedings of the International Conference on Materials in Oceanic Environment EUROMAT 98, Lisbon, July 1998, edited by. L. Faria (SPM, FEMS, Lisbon, 1998) p. 217.
5. I. MADARIAGA, I. GUTIÉRREZ, C. GARCÍA DE ANDRÉS and C. CAPDEVILA, *Scripta Mater.* **41** (1999) 229.
6. I. MADARIAGA and I. GUTIÉRREZ, in Proceedings of the Congreso Nacional de Tratamientos Térmicos y de Superficie TRATERMAT 98, Madrid, May 1998, edited by M. Carsi, F. Peñalba, O. A. Ruano and B. Fernandez (CENIM (CSIC), Madrid, 1998) p. 142.
7. J. R. YANG and H. K. D. H. BHADESHIA, in Proceedings of the International Conference in Welding Metallurgy of Structural Steels, Warrendale, PA, 1998 (TMS-AIME) p. 549.
8. M. STRANGWOOD and H. K. D. H. BHADESHIA, in "Advances in Welding Science and Technology," edited by S. A. David (ASM, Metals Park, OH, 1987) p. 209.
9. Y. ITO, M. NAKANASHI and Y. KOMIZO, *Met. Const.* **14** (1982) 472.
10. S. S. BABU and H. K. D. H. BHADESHIA, *Mater. Sci. Technol.* **6** (1990) 1005.
11. P. L. HARRISON and R. A. FARRAR, *Int. Mater. Rev.* **34** (1989) 35.
12. UNDERWOOD, in "Quantitative Stereology" (Addison-Wesley Publishing Co. Reading, 1970).
13. C. GARCÍA DE ANDRÉS, G. CARUANA and L. F. ÁLVARÉZ, *Mat. Sci. Eng.* **A241** (1998) 211.
14. G. F. VANDER VOORT, in "Metallographic Principles and Practice" (McGraw-Hill Book Co., NY, 1984) p. 427.
15. T. GLADMAN and F. G. PICKERING, *J. Iron Steel Inst.* **205** (1967) 653.
16. F. J. HUMPHREYS and M. HATHERLY, in "Recrystallization and Related Annealing Phenomena" (Pergamon, Oxford, 1995).
17. I. ANDERSEN, O. GRONG and N. RYUM, *Acta Mater.* **43** (1995) 2689.
18. G. N. HASSOLD and D. J. SROLOVITZ, *Scripta Mater.* **32** (1995) 1541.
19. H. K. D. H. BHADESHIA, in "Bainite in Steels" (The Institute of Materials, London, 1992) p. 33.
20. R. W. K. HONEYCOMBE and H. K. D. H. BHADESHIA, in "Steels: Microstructures and Properties" (E. Arnold Ltd., London, 1995) p. 152.
21. S. S. BABU and H. K. D. H. BHADESHIA, *Matter. Sci. Eng.* **A156** (1992) 1.
22. J. M. GREGG and H. K. D. H. BHADESHIA, *Acta Mater.* **45** (1997) 739.